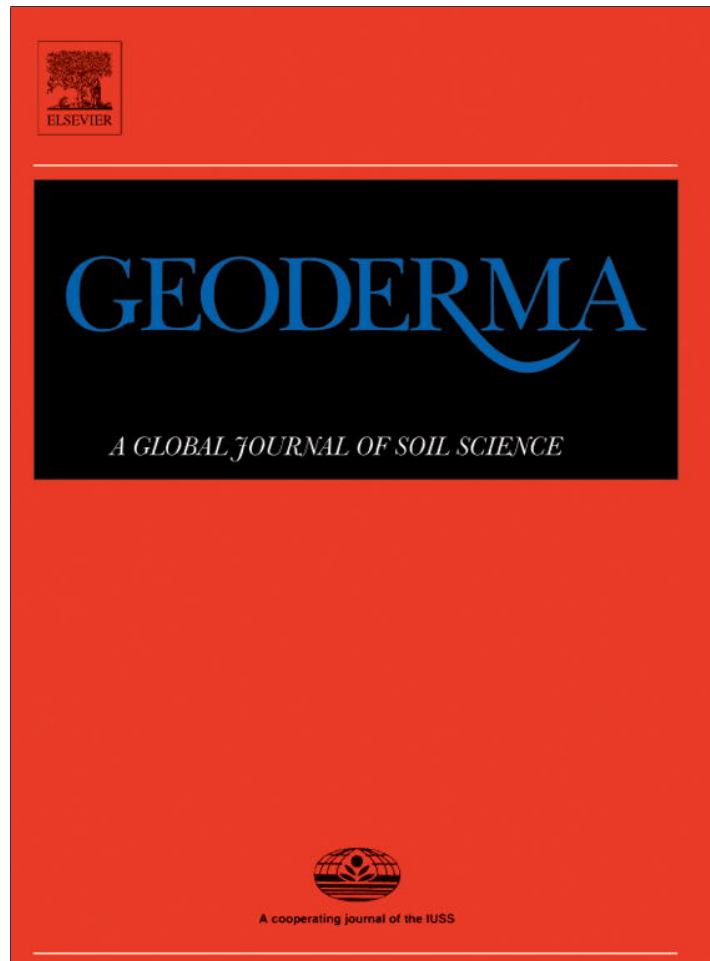


Provided for non-commercial research and education use.
Not for reproduction, distribution or commercial use.



(This is a sample cover image for this issue. The actual cover is not yet available at this time.)

This article appeared in a journal published by Elsevier. The attached copy is furnished to the author for internal non-commercial research and education use, including for instruction at the authors institution and sharing with colleagues.

Other uses, including reproduction and distribution, or selling or licensing copies, or posting to personal, institutional or third party websites are prohibited.

In most cases authors are permitted to post their version of the article (e.g. in Word or Tex form) to their personal website or institutional repository. Authors requiring further information regarding Elsevier's archiving and manuscript policies are encouraged to visit:

<http://www.elsevier.com/copyright>



Contents lists available at SciVerse ScienceDirect

Geoderma

journal homepage: www.elsevier.com/locate/geoderma

Soil prediction using artificial neural networks and topographic attributes

Claudinei Taborda Silveira ^{a,*}, Chisato Oka-Fiori ^a, Leonardo José Cordeiro Santos ^a, Angelo Evaristo Sirtoli ^b, Claudionor Ribeiro Silva ^c, Mosar Faria Botelho ^d

^a Departamento de Geografia, Setor de Ciências da Terra, Universidade Federal do Paraná, Curitiba, Brazil

^b Departamento de Solos, Setor de Ciências Agrárias, Universidade Federal do Paraná, Curitiba, Brazil

^c Instituto de Geografia, Universidade Federal de Uberlândia, Campus Monte Carmelo, Brazil

^d Universidade Tecnológica Federal do Paraná, Campus Dois Visinhos, Brazil

ARTICLE INFO

Article history:

Received 23 August 2011

Received in revised form 9 November 2012

Accepted 20 November 2012

Available online xxxx

Keywords:

Pedometry

Pedological cartography

Relief

DTM

ABSTRACT

Because relief maps show a strict relationship with soils at different spatial levels, distributions of soil units can be inferred from digital topography analyses. Geoprocessing techniques can be used to create parametric relief representations from digital terrain models (DTMs), and these models can be used to calculate primary and secondary topographical attributes, such as the elevation, profile and plan curvature, slope, stream power index, topographic wetness index, and sediment transport index. The classic method of pedological cartography is onerous and time-consuming; as an alternative, pedometric techniques favor the recognition of preliminary mapping units. In this study, a multilayered *perceptron* artificial neural network (ANN) with an error *backpropagation* algorithm was used, where topographical and geological attributes were used as input parameters. The classified map was validated by comparison with two preexisting conventional ground maps of the study area. The kappa (K) index, global exactness (GE), and exactness from the point of view of the producer and user were considered in the comparison. The quality of the soil units classified by the ANN was satisfactory, based on the K and GE values from the comparison.

© 2012 Published by Elsevier B.V.

1. Introduction

Despite a large demand for pedological cartography in Brazil, principally at detailed levels, several factors, such as the high cost of surveys, the vast territorial extent of areas to be mapped, and the difficulty of accessing certain areas, limit its application. Furthermore, the precision of information, the trustworthiness of qualitative interpretations, and the difficulty of extrapolating information to other areas pose challenges (Mendonça-Santos and Santos, 2003).

According to Santos (2007), only 35% of soils in the whole of Brazil have been mapped at exploratory and schematic levels (scales from 1:1,000,000 to 1:5,000,000) or at medium and small scales (1:100,000 to 1:600,000).

Currently, several methods are used to assist pedological cartography. These tools offer support for larger scale ground mapping, facilitate the determination of more precise unit limits, and provide more efficiency with lower financial costs. One such method is the digital mapping of reliefs, which uses quantitative techniques to predict soil-mapping units.

Digital techniques are becoming more prevalent as a result of advances in informatics that allow for rapid, accessible applications

of existing mathematical and statistical methods being used by soil scientists for the last few decades (McBratney et al., 2003).

New methods for digital ground mapping are being rapidly developed. Two main groups of auxiliary techniques have played an important role: a) orbital remote sensing images and b) topographic attributes derived from digital terrain models (DTMs) (Dobos et al., 2000). The latter method is used to identify homogeneous landscape units, which are supported in morphological relief models calculated from DTMs. It can be used to predict ground mapping because the positions of the soils in the section influence the pedogenic processes. Thus, topographic attributes can be applied to distinguish between pedological classes.

Relief digital modeling is one of the most common quantitative techniques used to predict soil attributes and classes (McKenzie et al., 2000). This method uses relief parameterization (Wood, 1996), where the primary and secondary topographic attributes are calculated, obtained in DTM.

The principal merit of digital terrain analysis is its support during the field work stage. This identification phase of preliminary units during data acquisition is supported by the use of a previously developed soil occurrence model (Ippoliti et al., 2005). Methodologies to predict soil units, derived from these standards, are efficient, increasing the speed of pedological surveys (Hermuche et al., 2002).

Researchers have shown that the spatial distribution of topographic attributes can be used to efficiently characterize relief morphology, that relief characteristics influence the distribution of soils,

* Corresponding author. Tel.: +55 41 9682 8816.

E-mail addresses: claudineits@ufpr.br (C.T. Silveira), chisato@ufpr.br (C. Oka-Fiori), santos@ufpr.br (L.J.C. Santos), sirtoli@ufpr.br (A.E. Sirtoli), crs.educ@gmail.com (C.R. Silva), mosar@ufpr.edu.br (M.F. Botelho).

and that predictive parametric soil models can aid pedological cartography.

It is worth highlighting experiments that were fundamental for this work. Zevenbergen and Thorne (1987) have shown the contribution of the quantitative analysis of land surface topography by using topographic indices. Klingebiel et al. (1987) employed geomorphologic variables in order to define soil units. Dikau (1989) has shown how the digital analysis of the terrain can be applied to the relief by using topographic feature quantification through the definition of basic unities for geomorphologic and pedologic mapping. Moore et al. (1991) have shown a set of primary and secondary topographic attributes obtained from digital terrain model for application in geomorphology and hydrology. Odeh et al. (1991) have verified that the variable slope, plan and profile curvature, extension of the slope and area of the top contributed to explain most of the variation of soils in their approach. Moore et al. (1993) have found significant correlation between the soil and the quantified terrain attributes whose variable slope and the wetness level showed greater correlation with the soil attributes. In the same perspective Gessler et al. (1995) have developed a statistic soil-landscape model, using different terrain attributes, such as: plan curvature and composed topographic index in order to estimate the soil characteristics. McKenzie and Ryan (1999) have employed environmental correlation as a method for spatial prediction of soil properties, and observed the relationship between the wetness and slope level with the density of the soil.

Recent works developed in Brazil that have contributed were those of Sirtoli et al. (2008a) who have shown relationships between the soil units and the relief attributes. Muñoz (2009) who presented the relationships between the geomorphometric variables obtained from the DEM SRTM90 with a pedologic data gathering on the scale of 1:100,000. Hermuche et al. (2002, 2003) have used the topographic attributes in RGB composition in order to define the soil units, later comparing them to a map on the scale of 1:50,000. Ippoliti et al. (2005) have identified geofoms and pedofoms through elevation, slope and curvature. Chagas (2006) has classified soil units with topographic attributes through ANN and the Maximum Likelihood classifier, comparing them to the conventional map on the scale of 1:50,000. Crivelenti (2009) has used the parameters of slope, plan and profile curvature, integrating them through trees of decision in order to make a map of soils in the scale of 1:50,000. Sirtoli et al. (2008b) have determined the soil units with a combination of the secondary topographic attributes and Silveira et al. (2012) have used stream power index, wetness index, and sediment transport index with slope, integrated through the means of crossed tabulation obtaining soil units that compared to a pre-existing map on the scale of 1:10,000 presented global accuracy 0.69 and coefficient Kappa 0.43.

Based on these observations, the objective of this research was to predict preliminary soil mapping units. The prediction was part of a digital relief analysis process that included seven topographical and geological attributes and was integrated into an artificial neural network (ANN).

ANNs provide advantages compared to image classifiers based on statistical concepts because no prior assumptions about the distribution of the data to be sorted are required (Sirtoli, 2008). Several studies have successfully used ANNs to support the identification of soil mapping units in Brazil (Chagas, 2006; Silveira, 2010; Sirtoli, 2008).

A study area that included the Corvo stream hydrographic basin was selected because it provided an adequate cartographic basis for the study objectives, with topographical maps at a 1:10,000 scale. Two conventional soil maps at 1:10,000 and 1:35,000 scales exist for this area, and these maps were used to validate the preliminary soil mapping units generated by the proposed method. The site has an area of 447.3 ha and is located in the city of Pinhais, in the state of Paraná, Brazil (Fig. 1).

The study area is situated in the Curitiba sediment basin, primarily in the Guabirotuba Formation and secondarily in the restricted plains

area of the Holocene sediments. The Guabirotuba Formation was formed in successive erosive phases. It is predominantly composed of green silt and clay deposits arranged in an interdigitated or abrupt gradation, depending on the local stratigraphic and structural characteristics, and is interlaced with arkosic sands and, occasionally, gravel; quartz pebble is predominant (Salamuni et al., 1999). The Holocene sediments are derived from the erosion and deposition of older weathered lithologies, formed by hydraulic-depositional conditioning of drainage from rivers and flood plains (Mineropar, 2001).

2. Method

2.1. Obtaining topographic attributes

A DTM was generated to represent the topographical elevation by extracting vectorial planialtimetric data from topographical sheets, at a scale of 1:10,000 (COMEC (Coordination of the Curitiba Metropolitan Region) (1976)). Other primary attributes, including the slope, profile and plan curvature, and secondary attributes, including the stream power index, wetness index, and sediment transport index, were derived from the DTM. These procedures were carried out using the software *MatLab* (Mathworks, 2007).

The topographic attribute extraction operations were executed using a movable window with nine cells (3×3) shifted sequentially on the total set of DTM data. This method calculates the parameters of a central cell while considering the surrounding cells (Fig. 2).

Slope was determined from the DTM using two local finite differences in the *x* and *y* directions (Horn, 1981):

$$\beta = \arctan\left(\sqrt{f_x^2 + f_y^2}\right) \quad (1)$$

where β represents the local inclination of the terrain, and f_x^2 and f_y^2 are approximations of the finite differences calculated by means of the partial derivatives f_x and f_y in the *x* and *y* directions (orthogonal to each other), respectively. The partial derivatives were determined by Eqs. (2) and (3), where λ is the width of each cell.

$$f_x = \frac{\partial z}{\partial x} = \frac{Z_6 - Z_4}{2\lambda} \quad (2)$$

$$f_y = \frac{\partial z}{\partial y} = \frac{Z_2 - Z_8}{2\lambda} \quad (3)$$

The profile curvature (φ) and plan curvature (ψ) were defined based on the finite difference values in the *x* and *y* directions (Moore et al., 1993; Zevenbergen and Thorne, 1987) and the second partial derivatives, as shown in Eqs. (4), (5) and (6).

$$f_{xx} = \frac{\partial^2 z}{\partial x^2} = \frac{Z_4 + Z_6 - 2Z_5}{\lambda^2} \quad (4)$$

$$f_{yy} = \frac{\partial^2 z}{\partial y^2} = \frac{Z_2 + Z_8 - 2Z_5}{\lambda^2} \quad (5)$$

$$f_{xy} = \frac{\partial^2 z}{\partial x \partial y} = \frac{-Z_1 + Z_3 + Z_7 - Z_9}{4\lambda^2} \quad (6)$$

Thus, the profile (φ) and plan curvature (ψ) were determined by Eqs. (7) and (8), respectively (Moore et al., 1993; Zevenbergen and Thorne, 1987).

$$\phi = \frac{-2(f_{xx}f_x^2 + f_{xy}f_xf_y + f_{yy}f_y^2)}{f_x^2 + f_y^2} \quad (7)$$

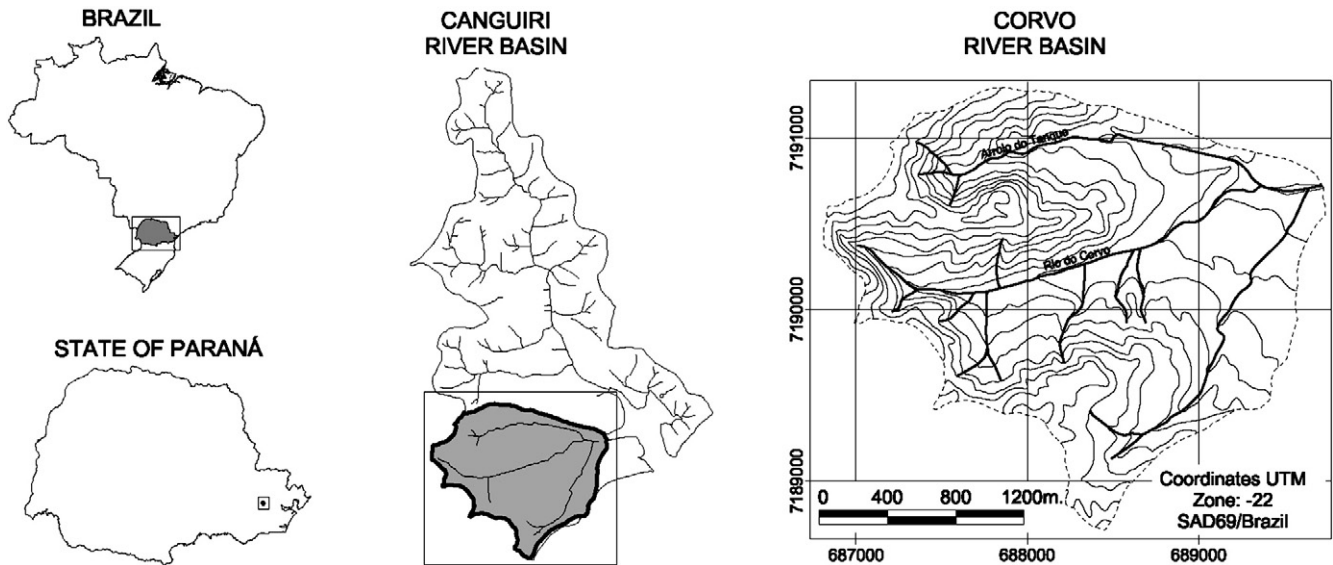


Fig. 1. Location of the study area.

$$\varpi = \frac{2(f_{xx}f_y^2 - f_{xy}f_xf_y + f_{yy}f_x^2)}{f_x^2 + f_y^2} \quad (8)$$

The stream power index (Ω) was defined as the product of the specific contribution area (A_c) and the tangent of the slope (β), according to Eq. (9) (Moore et al., 1991).

$$\Omega = A_c \tan \beta \quad (9)$$

where A_c is the specific area of contribution for the central point of the window (Eq. (10)).

$$A_c = (3\lambda^2) \quad (10)$$

The wetness index is defined by the natural logarithm of the ratio between the contribution area (A_c) and the tangent of the slope (in degrees), according to Eq. (11) (Moore et al., 1991).

$$w = \ln\left(\frac{A_c}{\tan \beta}\right) \quad (11)$$

Z_1	Z_2	Z_3
Z_4	Z_5	Z_6
Z_7	Z_8	Z_9

Fig. 2. Window with nine cells (3×3).

The variables considered in the sediment transport index (τ) were the specific contribution area (A_c) and the sine of the slope $\sin \beta$, described in Eq. (12) (Moore et al., 1991).

$$\tau = \left(\frac{A_c}{22.13}\right)^m \left(\frac{\sin \beta}{0.0896}\right)^n \quad (12)$$

The values of the constants m and n are 0.6 and 1.3, respectively.

2.2. Architecture and structure of the ANN

The ANN used to classify the preliminary soil mapping units, by means of the *MatLab* module *Neural Network Toolbox* (Mathworks, 2007), is composed of four layers: 1) an input layer with eight neurons that correspond to the seven topographical variables: elevation, slope, profile and plan curvature, stream power index, wetness index and sediment transport index, as well as the variable geology; 2) a first hidden intermediate layer with 130 neurons, a number determined through trial and error, as suggested by Hirose et al. (1991), by adding or removing neurons in the hidden layers based on the behavior of the error during the training phase; 3) a second hidden layer with 43 neurons, a number determined by observing the Hilton rule (1989), which states that, in the case of two intermediate layers, the number of second-layer neurons should not be greater than one-third of the number of neurons in the first; and 4) an output layer with three neurons that represent the soil classes.

The ANN uses a multilayer perceptron *feed-forward* architecture with a sigmoidal transference function and a learning logarithm for the backpropagation of error, *resilient propagation variation* (RPROP). In this algorithm, the weights of the connections are adjusted by feedback until convergence is achieved, where this determines the backpropagation of the error. Two steps are executed in the different net layers: “one step forward”, or propagation, and “one step backwards”, or backpropagation. In the propagation step, the weights of the connections are fixed. In the backpropagation step, the synaptic weights are adjusted by an error correction rule that consists of the difference between the output response of the network layer in question and the desired response. This produces an error signal, which is propagated backwards by means of the network in a direction opposite to that of the synaptic connections (Haykin, 2001).

The RPROP variation was developed by Reidmiller and Braun (1993) to minimize oscillations in the weight adjustments during ANN training and to achieve the lowest number of iterations and

the smallest average quadratic error (AQE) (Ribeiro, 2003). In this research, the threshold adopted for the AQE was 0.001.

For Chagas (2006), determining the learning rate for a specific problem is not a simple task because the most typically used values are in the range of 0.1 to 1.0. In this study, the learning rate was determined with a minimum value of 0.1, corresponding to the maximum number of iterations, 15,000. The real-time rate of errors committed during learning (“momentum”) must be at least 0.09, and the learning error (“performance”) must be less than 0.0001.

2.3. Validation of the preliminary soil mapping units

The preliminary soil mapping units classified by the ANN were validated by comparison with two preexisting soil maps, which were generated using conventional techniques. These maps, which covered the entire study area, were produced by Rocha (1990) at a 1:10,000 scale (Fig. 3-A) and by LIMA (2005) at a 1:35,000 scale (Fig. 3-B).

The results were quantitatively measured by error matrix analysis using the kappa index and the global exactness (GE) and accuracy from the points of view of the user and the producer. Qualitative interpretations of the kappa coefficient were based on ranges that represent image quality, according to Landis and Koch (1977) (Table 1).

3. Results and discussion

Based on the topographic attributes of the study area, the measured elevation, slope (α), topographic wetness index (w), stream power index (Ω), sediment transport index (τ), plan curvature (ψ), and profile curvature (φ) values varied between 884 and 954 m above sea level, 0 and 50%, 6 and 26, 0 and 118, 0 and 34, -1.814 and 1.410 , and -1.051 and $1.154^\circ/\text{m}$ respectively. Fig. 4 shows the frequency histogram of these attributes.

Based on the network trained with the best combination of variables according to Silveira (2010), the parameters were applied to the entire data set during simulation of the ANN, and three preliminary soil classes in the basin were delineated: Oxisols, Inceptisols, and Histosols + Gleys (Fig. 5).

Table 1
Image classification quality according to kappa index intervals.
Source: Adapted from Landis and Koch (1977).

Kappa coefficient	Image quality
Less than 0	Very poor
0.01–0.20	Poor
0.21–0.40	Reasonable
0.41–0.60	Good
0.61–0.80	Very good
0.81–1.00	Excellent

The preliminary soil map, classified by the ANN, was compared with two existing soil maps of the area to validate the classification. Two comparative sets were distinguished, comparison 1 and comparison 2. In the first, the preliminary map was overlaid and analyzed with pre-existing map 1; in the second, the map was overlaid and analyzed with pre-existing map 2.

Comparison 1 showed the greatest similarity, with 72% agreement between the mapped units, whereas comparison 2 showed 65% agreement. The kappa coefficient values obtained in the two comparisons indicated good quality, according to the quality classes presented by Landis and Koch (1977) (Table 1). The kappa values were 0.56 and 0.48 for preexisting maps 1 and 2, respectively.

From the error matrices, percentage values were obtained for user (UE) and producer (PE) exactness between the classes; the map classified by the ANN represented the producer's point of view, and the pre-existing maps represented the user's point of view.

In the error matrix for comparison 1 (Table 2), the classified units have elevated PE and UE values. The errors were not concentrated in any single class; thus, the soil units classified by the ANN did not differ from those of preexisting map 1, except for a divergence in the delineated limits associated with the proper pedological traditional cartography, in which spatial units are determined by a discrete model of spatial variability. In this model, soil type is assumed to change abruptly, which does not occur in reality because the variations are gradual. Subjectivity in the tracing of limits between soil units, therefore, differentiates the units of map 1 from those classified by the ANN. The results of the verified unconformities were small

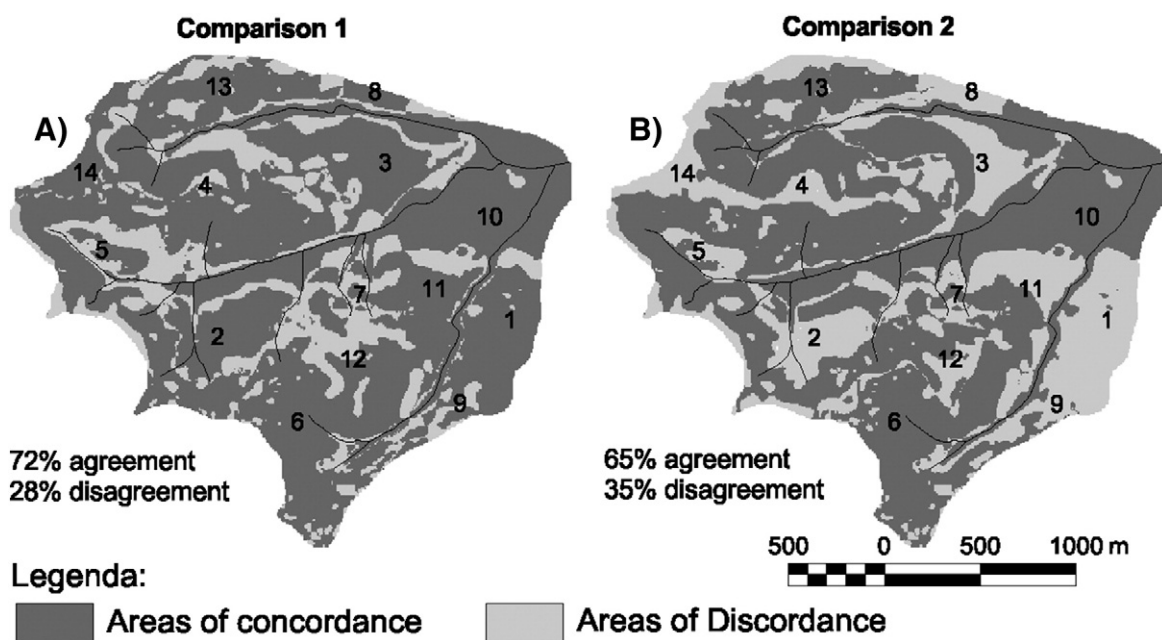


Fig. 3. Pre-existing soil mappings at the order level.

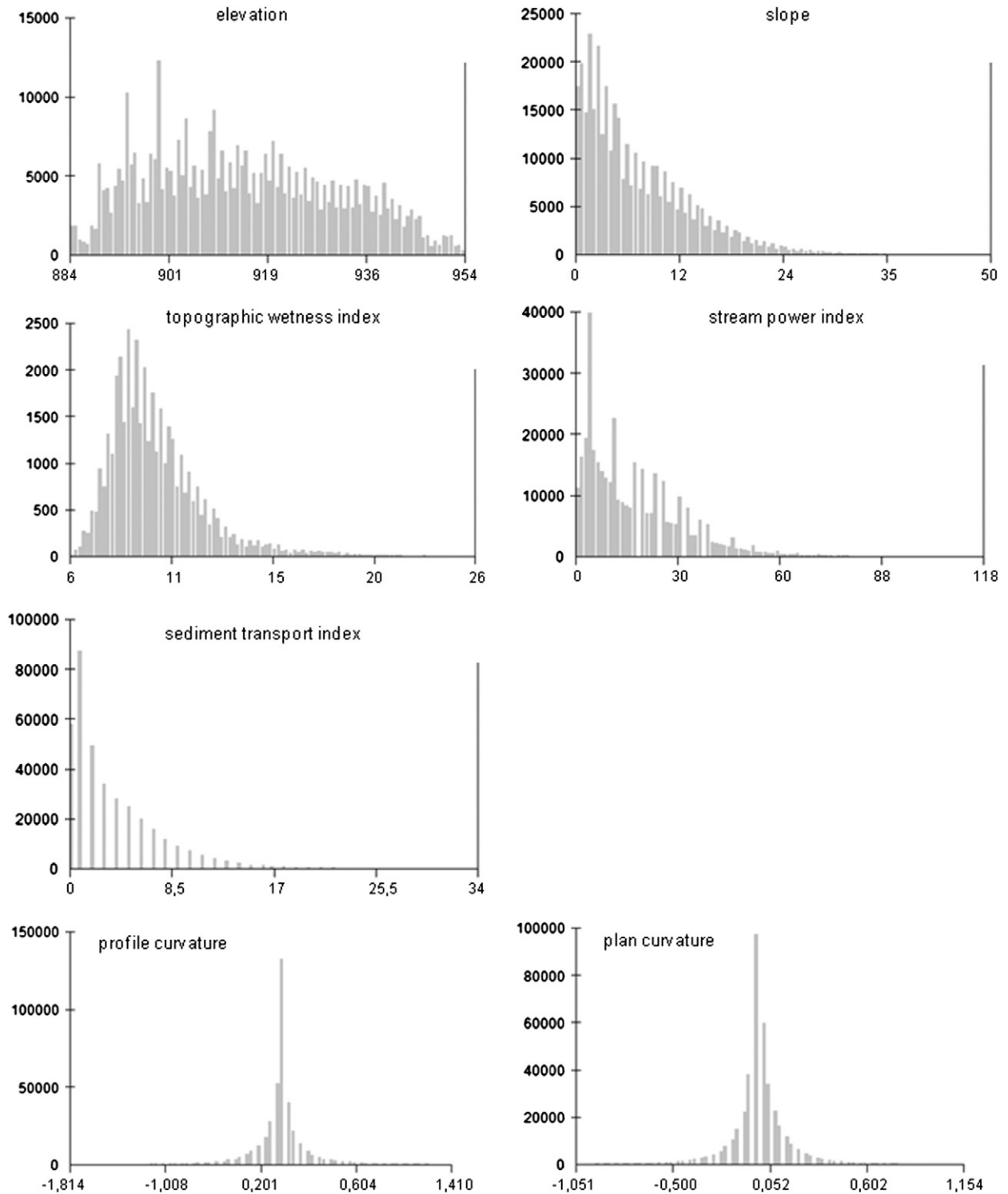


Fig. 4. Frequency histogram of the topographic attributes.

polygons that represented areas with interpretation divergence (Fig. 6-A).

In the error matrix of comparison 2 (Table 3), the divergences are concentrated mainly in the Oxisol class, with a low PE (39%), and the Histosol + Gley class, with a low UE (57%). The low exactness of the Oxisol class was associated with the disagreements shown in regions 1, 3, 8, 9, and 11 (Fig. 6-B), in which interpretations were conflicting. In pre-existing map 2, these areas represent the Histosol + Gley class,

and in the map classified by the network, they represent Oxisols. These disagreements are associated with the generalization of scale shown in comparison 2. Here, the hydromorphic soil limits were overestimated, resulting in low UE values for this class.

Other nonconformities between the maps correspond to non-mapped areas, such as Lima's (2005) interpretation of Oxisols in the top position of map 2 (regions 4 and 14) as Inceptisols due to the presence of elevated clay activity values in the analyzed samples.

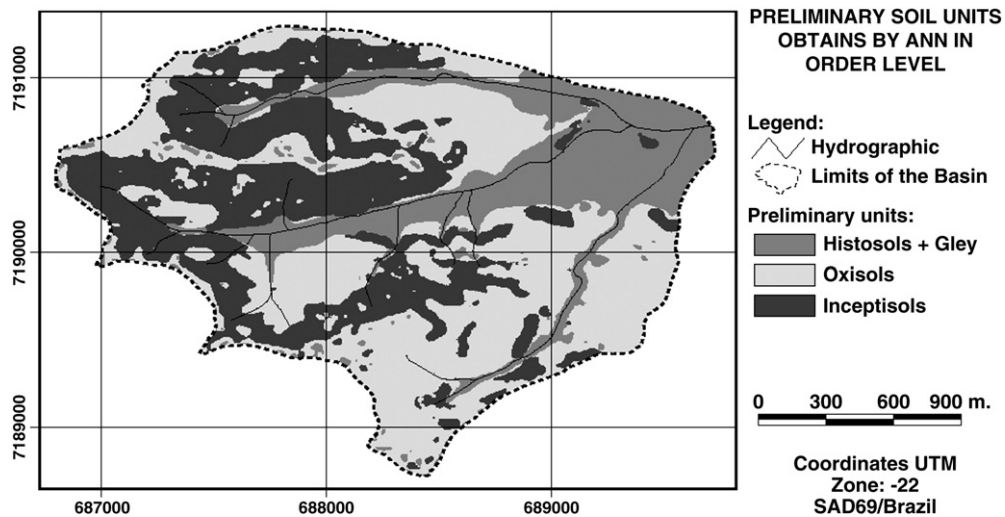


Fig. 5. Map of the preliminary soil mapping units classified by the ANN.

Table 2
 Error matrix from comparison 1.

Soil class		Preexisting conventional mapping 1			
		Histosols + Gleys	Oxisols	Inceptisols	PE
Mapping classified by the ANN	Histosols + Gleys	30,243	6412	2958	76%
	Oxisols	3858	60,649	14,194	77%
	Inceptisols	3172	19,693	37,909	62%
	UE	81%	70%	69%	GE = 0.72

Legend: PE – producer exactness; UE – user exactness; GE – global exactness.

However, the author of this mapping emphasized that the morphologic characteristics of this soil are similar to those of Oxisols. The other verified disagreements were associated with the degree of accuracy attained in tracing the limits of the classes between the comparative maps.

When analyzing the inclusion and omission errors of the classes mapped by the ANN compared to those of preexisting maps 1 and 2 (Table 4), the Inceptisol class exhibited an average inclusion error (In. E.) of 0.28 and an average omission error (Om. E.) of 0.33. The lowest In. E. and Om. E. of the Inceptisol class were in mapping 2 (0.17) and mapping 1 (0.31), respectively. These values demonstrate the efficiency of the unit mapping prediction.

In the Oxisol class, the average In. E. and Om. E. values, obtained in the comparison with the pre-existing soil maps, are 0.42 and 0.28, respectively (Table 4). The average inclusion value is greater than that verified in the Inceptisol class. However, this was a result of the elevated In. E. value of 0.61 obtained from map 2. In map 2, the limits of this unit were underestimated, and the hydromorphic character of the soils was not mapped in the interfluvials or at the tops of the slopes. In map 1, the principal divergence was linked to the contour limits between the classes.

The lowest average In. E. value of 0.19 was found in the Histosol + Gley class (Table 4), demonstrating that the classified limits of this

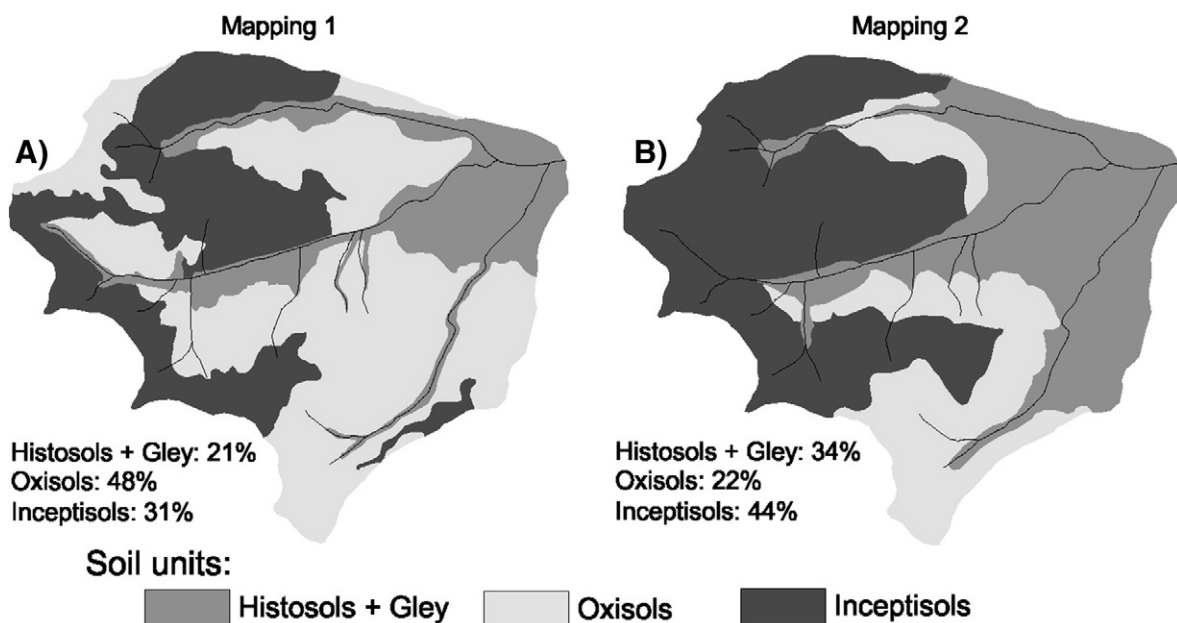


Fig. 6. Comparison between the preliminary soil units and pre-existing maps 1 and 2.

Table 3
Error matrix for comparison 2.

		Ground class	Preexisting conventional mapping 2			
			Histosols + Gleys	Oxisols	Inceptisols	PE
Mapping classified by the ANN	Histosols + Gleys	34,567	2774	2208	87%	
	Oxisols	22,910	30,364	25,286	39%	
	Inceptisols	2906	7148	50,605	83%	
	UE	57%	75%	65%	GE = 0.64	

Legend: PE – producer exactness; UE – user exactness; GE – global exactness.

Table 4
Errors of inclusion and omission between the preliminary units and the preexisting maps.

		Units	Preexisting mapping 1		Preexisting mapping 2		Average	
			In. E.	Om. E.	In. E.	Om. E.	In. E.	Om. E.
			Mapping classified by the ANN	Histosols + Gleys	0.38	0.31	0.17	0.35
	Oxisols	0.23	0.30	0.61	0.25	0.42	0.28	
	Inceptisols	0.24	0.19	0.13	0.43	0.19	0.31	

Legend: In. E. – inclusion error; Om. E. – omission error.

class were not overestimated on the conventional maps. Map 2 presented the poorest Om. E. results (0.43) due to the generalization of the Histosol + Gley class delimitation, a problem not associated with scale differences.

In validating the units predicted by the ANN, the classified soil map was shown to be adequate in comparison with the pre-existing conventional maps, with justified exceptions, principally in the determination of necessary limits between units. The classes determined by the ANN were shown to be satisfactory in the validation process relative to the pre-existing conventional maps.

A third comparison was carried out considering the differences between the pre-existing soil maps. The obtained GE and kappa coefficient values were 0.63 and 0.46, respectively, which, according to the Landis and Koch classification (1977), signifies good correspondence between the compared images.

The error matrix of comparison 3 (Table 5) shows exactness values of the classes from pre-existing map 1 in relation to the same classes from pre-existing map 2 (ExClsMp1-2) and of map 2 in relation to map 1 (ExClsMp2-1). The lowest matrix value of 37% was for the Oxisol of the ExClsMp1-2; however, this class in the ExClsMp2-1 had a value of 79%. This was due to the identification of a larger area of Oxisols (48% of the basin) in map 1 as compared to map 2 (22% of the basin). In the first map, this soil class includes the peaks and lower thirds of the slopes and the intermediate positions of the relief with less slope (Fig. 3-A). In the second map, these soils are more restricted to the lower third of the slopes (Fig. 3-B). Consequently, the areas of the Inceptisol and Histosol + Gley classes are larger in map 2, representing 44% and 34% of the basin, respectively. In map 1, these classes correspond to 31% and 21% of the area, respectively. Thus, these two soil classes caused

Table 5
Error matrix of comparison 3.

	Ground class	Conventional mapping 2			
		Histosols + Gleys	Oxisols	Inceptisols	ExClsMp1-2
Conventional mapping 1	Histosols + Gleys	32,529	3059	1669	87%
	Oxisols	25,871	31,941	28,843	37%
	Inceptisols	1983	5285	47,586	87%
	ExClsMp2-1	54%	79%	61%	GE = 0.63

Legend: ExClsMp1-2 – exactness of the classes in mapping 1 in relation to the same class of mapping 2; ExClsMp2-1 – exactness of the classes in mapping 2 in relation to the same class of mapping 1; GE – global exactness comparison 1.

the low values of the error matrix of ExClsMp2-1, with 54% in the Histosol + Gley class and 61% in the C class.

From the overlapping of the two maps, the divergence found in region 14 (Fig. 7) corresponded to the disagreement of Oxisols situated in the top position of mapping 1 in relation to mapping 2, where the soil was classified as Inceptisols. According to the author of map 2, the watersheds in the basin were relatively narrow; therefore, this area does not exhibit conditions for more evolved soil formations, such as Oxisols, despite similar morphological characteristics (LIMA, 2005). Thus, the Oxisols located in the watersheds of map 1 (Fig. 3-A) are not present in map 2 (Fig. 3-B).

The disagreements verified in regions 1, 3, 8, 9, and 11 were a result of the discordant interpretations of Oxisol in map 1 for the Histosol + Gley class in map 2, where regions 2 and 5, classified as Oxisols in map 1, are Inceptisols in map 2 (Fig. 6). The conflicts evidenced in these regions may be associated with differences in map scale and, therefore, in the level of detail; map 1 has a scale of 1:10,000, whereas map 2 has a scale of 1:35,000.

4. Conclusions

The use of ANN demonstrated potential in classifying preliminary soil mapping units using geomorphometry techniques.

During the validation step, the areas for which the mapped units diverged from the pre-existing maps were determined to be located in the peak and watershed positions. These areas were classified as small-class polygons of Histosol + Gley soils in areas of predominantly Oxisol soils, and small Inceptisol polygons in areas of predominantly Histosol + Gley soils. The inconsistencies identified in the predictions at the peaks and valley depths were associated with the degree of cartographic generalization at the 1:10,000 scale, which does not allow for the altimetric representation of intermediate values to within 5 m of the vertical equidistance between level curves. However, the use of variable geology contributed to a more accurate delimitation of the mapping units in these areas.

In the comparison between the ANN classification and the pre-existing mappings, the ANN map showed greater similarity to mapping 1 (comparison 1), with GE and kappa values of 0.72 and 0.56, respectively. The two conventional maps showed less agreement, with GE and kappa values of 0.77 and 0.65, respectively.

The advantages of the ANN classification included the following: a) decreased subjectivity in the determination of limits between mapping units; b) the ability to consider a greater number of classification variables; c) elimination of the need for pre-existing ground mappings in the study area or in contiguous areas with equivalent environmental characteristics to guide the understanding of relations between the soil and the landscape; d) elimination of the need to discretize the topographic attributes in a class to assess relationships with already mapped soil units (i.e., the formulation of prior hypotheses is unnecessary); e) assignment of random weights based on training samples, which reduces errors in the operation process; and f) the ability to use the tested network architecture application to predict soil units in homologous regions.

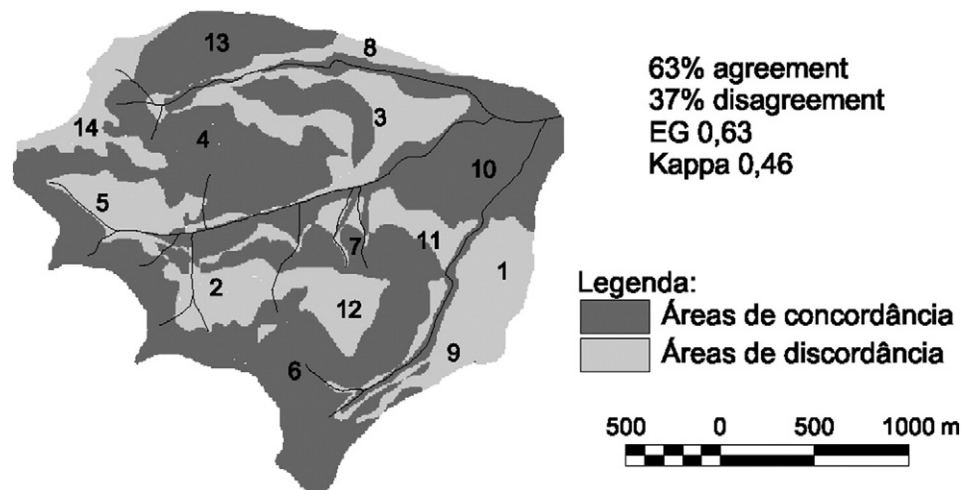


Fig. 7. Analysis of agreement between the pre-existing soil maps.

References

- Chagas, C.S., 2006. Digital Mapping of Soils by Environmental Correlation and Neural Networks in a Watershed in the Sea Hills Area. Ph.D. Dissertation, Federal University of Viçosa, Viçosa, Brazil.
- COMEC (Coordination of the Curitiba Metropolitan Region), 1976. Topographical maps, folhas: SG-22-X-D-I-4-SO-B e SG-22-X-D-I-4-SE-A, scale 1:10000.
- Crivellini, R.C., 2009. Data Mining to Infer the Soil-Landscape Relation in Digital Mapping of Soil. Ph.D. Dissertation, Agronomic Institute, Campinas, Brazil.
- Dikau, R., 1989. The application of a digital relief model to landform analysis in geomorphology. In: Raper, J. (Ed.), Three Dimensional Applications in Geographic Information Systems. Taylor and Francis, New York, pp. 51–77.
- Dobos, E., Micheli, E., Baumgardner, M.F., Biehl, L., Helt, T., 2000. Use of combined digital elevation model and satellite radiometric data for regional soil mapping. *Geoderma* 97, 367–391.
- Gessler, P.E., Moore, I.D., McKenzie, N.J., Ryan, P.J., 1995. Soil landscape modeling and spatial prediction of soil attributes. *International Journal of Geographical Information Systems* 9 (4), 421–432.
- Haykin, S., 2001. *Neural Networks: Principles and Practice*, second ed. Bookman, Porto Alegre, Brazil.
- Hermuche, P.M., Guimarães, R.F., Carvalho, A.P.F., Martins, E.S., Druck, S., Carvalho Júnior, O.A., Santos, N.B.F., Reatto, A., 2002. Morphometry as support for pedological map elaboration: I. Asymmetric water basins. *Brazilian Agricultural Studies Company – Embrapa, Planaltina, Brazil*, Document 68.
- Hermuche, P.M., Andrade, A.C., Guimarães, R.F., Leal Carvalho Júnior, O.A., Martins, E.S., 2003. Geomorphological subdivision on a regional scale of the Paraná river basin. *Brazilian Symposium of Applied Physical Geography*, X, 2003, Rio de Janeiro. SBGFA, Anais... Rio de Janeiro.
- Hilton, G.E., 1989. Connectionist learning procedures. *Artificial Intelligence* 40, 185–234.
- Hirose, Y., Yamashita, K., Hijiya, S., 1991. Back-propagation algorithm which varies the number of hidden units. *Neural Networks* 4, 61–66.
- Horn, B.K.P., 1981. Hill shading and the reflectance map. *Proceedings of the Institute of Electrical and Electronic Engineers* 69, 14–47.
- Ippoliti, G.A., Costa, L.M., Schaefer, C.E.G.R., Fernandes Filho, E.I., Gaggero, M.R., Souza, E., 2005. Digital analysis of terrain: tool in the identification of landforms in the microbasin in the “Mar de Morros” region (MG). *Revista Brasileira de Ciência do Solo* 29, 269–276.
- Klingebiel, A.A., Horvarth, E.H., Moore, D.G., Reybold, W.U., 1987. Use of slope, aspect, and elevation maps derived from digital elevation model data in making soil surveys. *Soil Science Society of America. SSSA Special Publication*, 20, pp. 77–90.
- Landis, J.R., Koch, G.G., 1977. The measurement of observer agreement for categorical data. *Biometrics* 33, 159–174.
- Lima, M.R., 2005. Attributes of Soils and Floating Aquatic Macrophytes: A Contribution to Agricultural and Environmental Sustainability in the Iraí River Basin (PR). Ph.D. Thesis, Federal University of Paraná, Curitiba, Brazil.
- Mathworks, 2007. *User's Guide – Neural Network Toolbox*, MatLab. Math Works.
- McBratney, A.B., Mendonça-Santos, M.L., Minasny, B., 2003. On digital soil mapping. *Geoderma* 117, 3–52.
- McKenzie, N.J., Ryan, P.J., 1999. Spatial prediction of soil properties using environmental correlation. *Geoderma* 89, 67–94.
- McKenzie, N.J., Gessler, P.E., Ryan, P.J., O'Connell, D., 2000. The role of terrain analysis in soil mapping. In: Wilson, J.P., Gallant, J.C. (Eds.), *Terrain Analysis: Principles and Applications*. Wiley, New York, pp. 245–265.
- Mendonça-Santos, M.L., Santos, H.G., 2003. Digital mapping of soil attributes and classes—methods, paradigms and new techniques. *Empresa Brasileira de Pesquisa Agropecuária – Embrapa, Rio de Janeiro, Brazil*, Document 55.
- Mineropar – Minerais do Paraná SA, 2001. *Geological Atlas of the State of Paraná*. Mineropar, Curitiba, Brazil.
- Moore, I.D., Grayson, R.B., Ladson, A.R., 1991. Digital terrain modeling: a review of hydrological, geomorphological and biological applications. *Hydrological Processes* 5, 3–30.
- Moore, I.D., Gessler, G.A., Peterson, G.A., 1993. Soil attribute prediction using terrain analysis. *Soil Science Society of America Journal* 57, 443–452.
- Muñoz, V.A., 2009. Geomorphometric Analysis of SRTM Data Applied to the Study of Soil-Relief Relationships. Master's Dissertation, National Institute of Spatial Research, São José dos Campos, Brazil.
- Odeh, I.O.A., Chittleborough, D.J., McBratney, A.B., 1991. Elucidation of soil-landform interrelationships by canonical ordination analysis. *Geoderma* 49, 1–32.
- Reidmiller, M., Braun, H., 1993. A direct adaptive method for faster backpropagation learning: the RPROP algorithm. *IEEE International Conference on Neural Networks (ICNN)*, San Francisco, CA, pp. 586–591.
- Ribeiro, S.R.A., 2003. Integration of Landsat TM Images and Auxiliary Data for the Automatic Delimitation of Physiognomic and Geological Units (Landscape) Using Artificial Neural Networks. Ph.D. Thesis, Federal University of Paraná, Curitiba, Brazil.
- Rocha, H.O., 1990. Preliminary map of the Canguiri Farm soils, scale 1:10000. *Impresso, Curitiba, Brazil*.
- Salamuni, E., Salamuni, R., Ebert, H.D., 1999. Contribution of the sediment basin to the geology of Curitiba (PR). *Geosciences Bulletin of Paraná* 47, 123–142.
- Santos, H.G., 2007. Importance and development of soil surveys in Brazil. *Informative Bulletin of the Brazilian Society for Soil Sciences* 32, 18–20.
- Silveira, C.T., 2010. Digital Analysis of Relief Units in Predicting Preliminary Soil Mapping: Integration of Topographic attributes in Geographic Information Systems and Artificial Neural Networks. Ph.D. Thesis, Federal University of Paraná, Curitiba, Brazil.
- Silveira, C.T., Oka-Fiori, C., Santos, L.J.C., Sirtoli, A.E., Silva, C.R., 2012. Pedometry supported in topographic attributes with operations of mapping algebra crossed tables. *Brazilian Journal of Geomorphology* 13 (2), 125–135.
- Sirtoli, A.E., 2008. Soil Mapping with the Help of Terrain Attributes, Spectral Indexes and Geology Integrated by Artificial Neural Networks. Ph.D. Thesis, Federal University of Paraná, Curitiba, Brazil.
- Sirtoli, A.E., Silveira, C.T., Montovani, L.E., Sirtoli, A.R.A., Oka-Fiori, C., 2008a. Relief attributes derived from digital elevation model and their relationships with soils. *Scientia Agrária* 9 (3), 317–329.
- Sirtoli, A.E., Silveira, C.T., Montovani, L.E., C. T., Silva, C.R., Ribeiro, S.R.A., Oka-Fiori, C., 2008b. Secondary topographic attributes in mapping pedoforms. *Geosciences* 21 (1), 63–77.
- Wood, J., 1996. The Geomorphological Characterization of Digital Elevation Models. Ph.D. Thesis, University of Leicester, Leicester, UK. Available at: <http://www.soil.city.ac.uk/~jwo/phd>.
- Zevenbergen, L.W., Thorne, C.R., 1987. Quantitative analysis of land surface topography. *Earth Surface Processes and Landforms* 12, 47–56.